THE JOURNAL OF PHYSICAL CHEMISTRY B

Article

pubs.acs.org/JPCB

Conformational Heterogeneity of Methyl 4-Hydroxycinnamate: A Gas-Phase UV−IR Spectroscopic Study

Eric M. M. Tan,[†] Saeed Amirjalayer,[†] Szymon Smolarek,[†] Alexander Vdovin,[†] Anouk M. Rijs,[‡] and Wybren J. Buma*[,†]

[†]Van't Hoff Institute for Molecular Sciences, Faculty of Science, University of Amsterdam, Science Park 904, 1098 XH Amsterdam, The Netherlands

[‡]Radboud University Nijmegen, Institute for Molecules and Materials, FELIX facility, Toernooiveld 7, 6525 ED Nijmegen, The Netherlands

Supporting Information

ABSTRACT: UV excitation and IR absorption spectroscopy on jet-cooled molecules is used to study the conformational heterogeneity of methyl 4-hydroxycinnamate, a model chromophore of the Photoactive Yellow Protein (PYP), and to determine the spectroscopic properties of the various conformers. UV−UV depletion spectroscopy identifies four different species with distinct electronic excitation spectra. Quantum chemical calculations argue that these species are associated with different conformers involving the s-*cis*/s-*trans* configuration of the ester with respect to the propenyl C−C single bond and the *syn*/*anti* orientation of the phenolic OH group. IR−UV hole-burning spectroscopy is used to record their IR absorption spectra in the fingerprint region. Comparison with IR absorption spectra predicted by quantum chemical calculations provides vibrational markers for each of the conformers, on the basis of which each of the species observed with UV−UV depletion spectroscopy is assigned. Although both DFT and wave function methods reproduce experimental frequencies, we find that calculations at the MP2 level are necessary to obtain agreement with experimentally observed intensities. To elucidate the role of the environment, we compare the IR spectra of the isolated conformers with IR spectra of methyl 4-hydroxycinnamate−water clusters, and with IR spectra of methyl 4-hydroxycinnamate in solution.

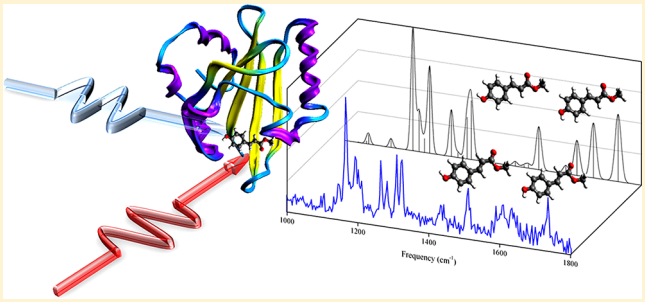

INTRODUCTION

Photoactive yellow protein (PYP), originally isolated from the *Halorhodospira halophila* bacterium[1,2] where it is responsible for the phototaxis toward blue light, is a small (14 kDa), water-soluble protein that can be crystallized easily and has a remarkable chemical and photo stability. Because of these favorable properties, PYP has become over the years a well-established model to study the conversion of photon energy into biological function.[3] The chromophore responsible for light absorption in PYP is deprotonated *p*-coumaric acid (*p*CA). It is therefore not surprising that the properties of the ground and electronically excited states of *p*CA and its derivatives have been the subject of a large number of theoretical[4−6] and experimental studies.[7−10] In the protein, *p*CA is covalently attached to a cysteine residue by a thioester bond. The ester functionality influences the structural and excited-state properties of the chromophore; studies of molecular systems such as methyl 4-hydroxycinnamate (historically indicated as OM*p*CA) in which this functionality is incorporated are therefore important to assess the influence of the protein environment. In previous LIF[11] and REMPI[12] studies on OM*p*CA, it was argued that under molecular beam expansion conditions one can expect the presence of four different conformers. These conformers involve the s-*cis* and s-*trans* configurations of the ester functionality around the propenyl C−C single bond (see Scheme 1). In addition, for each of these conformers the phenolic OH group can adopt a *syn* or *anti* configuration. UV−UV depletion and UV−UV hole burning spectroscopies indeed confirmed the presence of three species, while a tentative proposal was made for the $S_1 \leftarrow S_0$ origin transition of the fourth species.[11]

Careful consideration of the excitation spectra of the various species shows that they exhibit small but pertinent differences. At the same time, recent studies of the excited-state dynamics of OM*p*CA and its hydrated complex in the time[13] and frequency domain[14] lead to the conclusion that also the excited-state dynamics and their dependence on excess energy in the excited state vary from conformer to conformer. Apart from elucidating the photophysical and photochemical properties of PYP, OM*p*CA thus also offers the possibility to study how relatively small differences in geometrical structure are translated into differences in electronic structure, and may

Received: December 21, 2012
Revised: March 29, 2013
Published: April 10, 2013

Scheme 1. Conformers of Methyl 4-Hydroxycinnamate (OM*p*CA) Considered in Present Study: (a) s-*cis* OH-*anti*, (b) s-*cis* OH-*syn*; (c) s-*trans* OH-*anti*; (d) s-*trans* OH-*syn*

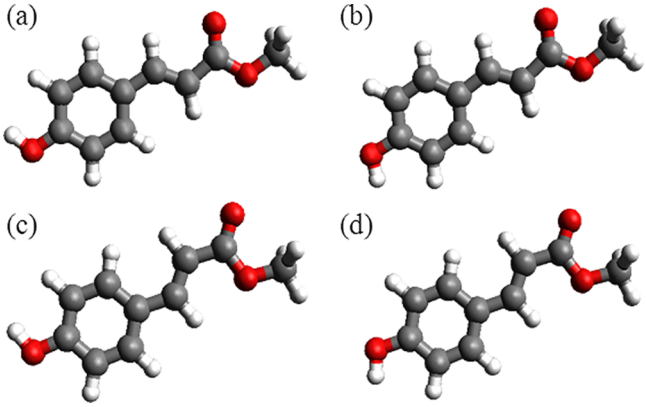

serve as a benchmark for detailed quantum chemical calculations. However, in order to fully exploit such a potential it is necessary to determine which conformer is associated with each of the species observed in the double-resonance studies.

Previously, such an assignment has been done on the basis of the results of CC2 and DFT quantum chemical calculations on OM*p*CA[11] and the analogy with *p*-vinylphenol (*p*VP).[15] Using a CC2 (DFT) approach the calculations predicted that the s-*cis* conformers are more stable than their corresponding s-*trans* conformers by 0.8 (0.9) kcal/mol. The same calculations found that *syn* and *anti* conformers differ only by 0.1 kcal/mol, the *anti* conformer formally being of lower energy. The $S_1 \leftarrow S_0$ excitation spectrum of *p*VP shows a similar *syn*/*anti* doublet as observed for OM*p*CA. For *p*VP, rotationally resolved fluorescence excitation spectroscopy[16] allowed an unambiguous assignment of the two components, the red- and blue-shifted members of the doublet assigned, respectively, to the *anti* and *syn* conformers. Combined with the observation that the intensity of *p*VP *anti* transitions in the $S_1 \leftarrow S_0$ excitation spectrum is about twice as large as those of *syn* transitions, it was concluded that the predicted stability ordering was correct, thus giving credence to an assignment of the *syn*/*anti* doublet in OM*p*CA using a similar intensity reasoning.

However, the reported energy differences for OM*p*CA—and certainly the energy difference between the *syn* and *anti* conformer—fall within the accuracy of these types of calculation. Similarly, the experimental comparison with *p*VP provides only indirectly an indication for an assignment. It is therefore clear that other means to come to an unambiguous assignment would be most welcome. In the present study, we employ to this purpose IR vibrational absorption spectroscopy. Such studies have been performed in the past in the 3 μm region,[12] but, as might be expected, the frequency of the phenolic OH stretch is within the accuracy of the measurements the same for all conformers (3651.7 cm^{-1}), and does not provide the means to distinguish them. In the present work, we have therefore recorded spectra in the fingerprint region (1000−1800 cm^{-1}) using a widely tunable infrared free electron laser. We will show that comparison with spectra predicted by various high-quality quantum chemical methods identifies several vibrational markers that serve to come to an assignment of the conformers. On the basis of these vibrational markers, it will also be concluded that the original assignment of UV−UV depletion spectra of the s-*cis* and s-*trans* conformers in the OM*p*CA-H_2O cluster should be reversed. The IR spectra recorded for the isolated molecule will furthermore be used to discuss the influence of a solvent and of the protein environment.

EXPERIMENTAL AND THEORETICAL DETAILS

REMPI spectroscopy and IR absorption measurements have been performed in two separate setups—in the following indicated as the Amsterdam and the FELIX facility setups—designed to perform laser spectroscopy on molecules cooled in a supersonic free jet expansion. For the present experiments, an injector assembly has been used to create the molecular beam that consists of a stainless-steel oven in which a glass container with the sample is placed, and a pulsed valve (General Valve) equipped with a 0.5 mm diameter nozzle. The pulsed valve is typically kept 10 °C above the oven temperature to prevent clogging of the nozzle. This injector assembly was incorporated in both the Amsterdam and FELIX facility setups into a differentially pumped setup equipped with a reflectron time-of-flight mass spectrometer (R.M. Jordan Co.) that has been described in detail previously.[17,18] In our experiments, methyl 4-hydroxycinnamate (ABCR, 95% purity) was heated to 165 °C and expanded with 3 bar of neon or argon as a carrier gas. The molecular beam was perpendicular to the depletion (pump) and ionization (probe) laser beams, while the electric field, which was applied to accelerate the ions along the time-of-flight mass spectrometer tube axis, was perpendicular to the molecular beam and laser beam axes.

UV−UV depletion spectroscopy has been performed with the Amsterdam setup using a two-color (1 + 1′) resonance enhanced two-photon ionization (RE2PI) scheme to generate an ion signal that served as probe. In order to produce this probe signal, a 30 Hz Nd:YAG (Spectra Physics Lab 190) pumped dye laser (Sirah Precision Scan) operating on a mixture of Rhodamine 610 and 640 and frequency-doubled by a KDP crystal was tuned to one of the transitions observed in the $S_1 \leftarrow S_0$ excitation spectrum, while an ArF excimer laser (Neweks PSX-501, 5 mJ per pulse) ionized the molecule from the S_1 state. The pump beam was obtained from a Lumonics HD500 dye laser operating on Rhodamine 640 and pumped by a XeCl excimer laser (Lambda Physik CompexPro 205). The time delay between pump and probe was 100 ns. Typical pulse energies for pump and $S_1 \leftarrow S_0$ excitation were 0.5−1.0 and 2−3 mJ, respectively. In the present study, a Burleigh WA-4500 wavemeter was used for the determination of the absolute wavelength of both dye lasers. Since in previous studies[11,12] the wavelength had been calibrated in an indirect manner, the excitation frequencies reported in the present study differ slightly from those frequencies.

IR−UV depletion spectroscopy with a one-color (1 + 1) RE2PI scheme and using the FELIX facility setup has been employed to record conformer-selective IR ground-state vibrational absorption spectra. In this setup, a dye laser (Radiant Dye, Narrowscan) pumped by a Nd:YAG laser ((Innolas GmbH, Spitlight 1200)) was used as the UV source. The dye laser was operating on a mixture of Rhodamine 610 and Rhodamine 640, and was frequency-doubled by a BBO crystal. The pulse energy of this UV beam was in the range of 2−3 mJ per pulse. For the generation of IR light in the frequency range between 1000 and 1800 cm^{-1}, we employed the Free Electron Laser for Infrared eXperiments (FELIX). FELIX produces pulses with a pulse duration of about 5 μs and pulse energies of about 100 mJ. The spectral line width is

dx.doi.org/10.1021/jp312624e | J. Phys. Chem. B 2013, 117, 4798−4805

typically 0.5% of the IR frequency. Both the molecular beam and the UV laser beam were running at 10 Hz, while FELIX was running at 5 Hz. In order to minimize signal fluctuations due to long-time drifts under the UV laser power or source conditions, a normalized ion-dip spectrum was obtained by recording separately the alternating IR-off and IR-on signals. IR spectra of OM*p*CA in solution with a spectral resolution of 2 cm^{-1} have been recorded with a Bruker Vertex 70 FTIR spectrometer.

In order to come to an unambiguous assignment of the measured IR absorption spectra to the various conformers, quantum chemical calculations have been performed on their equilibrium geometry and harmonic force fields with both density functional theory (DFT) as well as wave function theory (WFT) methods. In agreement with the experimental observations, we found in exploratory calculations that the differences between the spectra of these conformers were rather subtle. Under such circumstances a proper choice of basis set becomes more important. We have therefore extensively assessed how features in the predicted spectra that enabled one to distinguish the various conformers depend on the choice of basis set. From these calculations it was concluded that for the present purposes the cc-pVTZ basis set[19] was adequate as it is relatively a large atomic orbital basis sets that can provide competitive accuracy of prediction, while at the same time it allowed us to achieve a consistent comparison between the various methods employed. A further issue of interest is the importance of a dispersion correction. To this purpose, methods have been tested that include popular density functionals like the Becke's three-parameter hybrid exchange functional[20] in combination with the Lee, Yang, and Parr correlation functional (B3LYP),[21] followed by B3LYP-D3, which was developed to include empirical dispersion correction.[22] Furthermore, wave function methods like standard MP2 and spin-component-scaled second-order Moller–Plesset, SCS-MP2,[23] have been used. Finally, one should consider as well the importance of anharmonicity. To assess how anharmonicity effects the IR spectra, we have performed for a number of computational approaches anharmonic calculations. However, in these calculations we find that the differences with the harmonic calculations are minimal (see Supporting Information). In view of the computational costs, we have therefore not pursued such anharmonic calculations for all types of calculations, and report here only the results of the harmonic calculations. All calculations have been performed with the TURBOMOLE 5.9 suite of programs.[24]

RESULTS AND DISCUSSION

A. UV Absorption Spectra of Methyl 4-Hydroxycinnamate Conformers. Figure 1a displays the two-color (1 + 1′) RE2PI excitation spectrum of OM*p*CA detected at the mass of the molecular ion (m/e = 178). Compared to the one-color RE2PI excitation spectrum reported in ref 12, one now observes significantly more narrow line widths, the excitation spectrum being in fact nearly identical to the LIF spectrum reported in ref 11. The reasons that in the present experiments more narrow line widths are obtained are 2-fold. First, in the configurations employed the Lumonics HD500 and Sirah PrecisionScan dye lasers have a different resolution. Second, the use of 193 nm to ionize the molecule from S_1 results in more efficient ionization than in the one-color scheme. As a result, a lower laser power can be employed for the $S_1 \leftarrow S_0$ transition, thereby avoiding partial saturation as was concluded to occur in the previous one-color RE2PI experiments.[12] Power-dependence studies indeed showed that under the presently employed conditions the signal was linearly dependent on the intensity of the laser used to pump the $S_1 \leftarrow S_0$ transition. In our previous experiments, we could only identify with certainty three of the four expected conformers. The more favorable experimental conditions employed here enable us to identify the fourth conformer as well, as can be seen in the UV–UV depletion spectra depicted in Figure 1b–e.

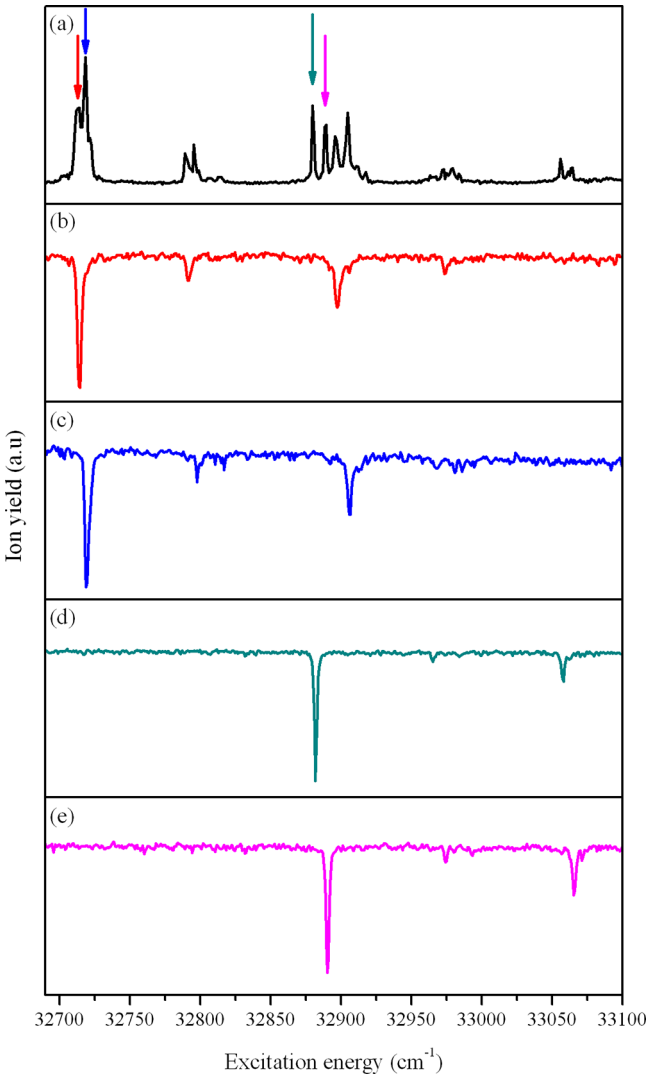

Figure 1. (a) (1 + 1′) RE2PI excitation spectrum of OM*p*CA. Spectra (b–e) display UV–UV ion depletion spectra obtained at the wavelengths indicated in spectrum (a). On the basis of their IR spectra (Figures 3–5), spectra (b–e) are assigned to the s-*cis* OH-*syn* (b), s-*cis* OH-*anti* (c), s-*trans* OH-*anti* (d), and s-*trans* OH-*syn* (e) conformers (see text).

The comparison of the four excitation spectra leads to a number of interesting observations. First, we find that the s-*cis* and s-*trans* conformers exhibit a different splitting between the origin transitions of the *syn* and *anti* conformers. For the s-*cis* conformer (traces b and c) a difference of 5.2 cm^{-1} is found, while this difference is 8.5 cm^{-1} for the s-*trans* conformer (traces d and e). Although these splittings are similar in magnitude to what is observed for analogous systems like *p*-vinylphenol[15] and *p*-coumaryl alcohol,[25] the relatively large difference between the two is remarkable and deserves further

dx.doi.org/10.1021/jp312624e | J. Phys. Chem. B 2013, 117, 4798–4805

theoretical attention. Second, for transitions associated with s-*cis* conformers, different line shapes and line widths are observed than for transitions associated with s-*trans* conformers. For the former the line shape appears to be asymmetric and may in fact reflect the onset of resolving a rotational band contour, while for the latter a symmetric line shape is found. Analogously, we find that the width of s-*trans* bands is systematically smaller than the width of s-*cis* bands.

B. IR Absorption Spectra of Methyl 4-Hydroxycinnamate Conformers. Figure 2a–c displays IR–UV depletion spectra obtained when setting the UV RE2PI laser frequency at 32 710.0, 32 720.0, and 32 871.0 cm^{-1}, respectively, and detecting at the mass of the molecular ion. As we will argue below, one can conclude from the IR spectra that these wavelengths are associated with the $S_1 \leftarrow S_0$ origin transitions of the s-*cis* OH-*syn*, s-*cis* OH-*anti*, and s-*trans* OH-*anti* conformers. Since in these experiments the probe signal was generated with a one-color RE2PI scheme, partial saturation could not be avoided (vide supra). Moreover, the resolution of the dye laser system used in the FELIX facility setup is not as good as the resolution of the dye laser system used in recording the UV–UV depletion spectra shown in Figure 1. The frequencies have therefore on purpose been chosen to the red, blue, and red side of the respective band maxima in order to avoid simultaneous probing of more than one conformer. Another consequence of the experimental conditions is that in the IR–UV experiments it was not possible to pump the $S_1 \leftarrow S_0$ origin transition of the fourth conformer (the s-*trans* OH-*syn* conformer) without also partially pumping the s-*cis* OH-*syn* conformer via the vibronic band at a slightly higher excitation energy.

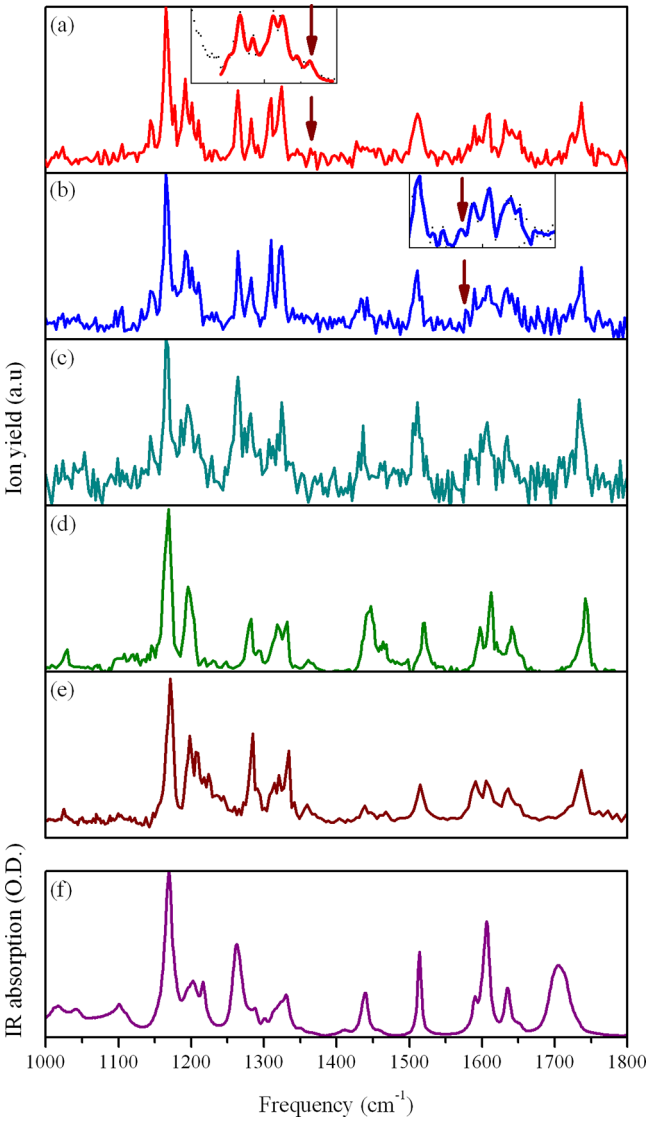

Figure 2. IR absorption spectra of various conformers of OM*p*CA (a–c) and of the OM*p*CA-H_2O cluster (d and e). Spectra (a–e) have been obtained with mass-selective IR–UV depletion experiments in which UV excitation occurred at (a) 32 710.0 cm^{-1} (s-*cis* OH-*syn* OM*p*CA), (b) 32 720.0 cm^{-1} (s-*cis* OH-*anti* OM*p*CA); (c) 32 871.0 cm^{-1} (s-*trans* OH-*anti* OM*p*CA); (d) 32 078.0 cm^{-1} (s-*cis* OM*p*CA-H_2O cluster); (e) 32 142.0 cm^{-1} (s-*trans* OM*p*CA-H_2O cluster). The insets in (a) and (b) have been recorded under higher IR intensity conditions in order to bring forward a number of low-intensity vibrational bands important for assigning the various conformers. The FTIR spectrum displayed in (f) has been obtained for OM*p*CA dissolved in chloroform at room temperature.

In order to relate the three IR–UV depletion spectra to specific conformers, we will in the following first discuss the results of quantum chemical calculations on their stability and vibrational spectra, and compare the performance of the various DFT and WFT methods. These predictions will then be used to assess which bands can be considered as unique markers for each of the conformers. Subsequently, we will show that such markers can indeed be identified in the experimental spectra, enabling a one-to-one assignment of IR spectrum to conformer. Finally, in order to assess the influence of a solvent environment, we will compare the experimental IR absorption spectra obtained in the gas phase with spectra obtained for the OM*p*CA-H_2O cluster and for OM*p*CA in solution.

Table 1 reports the relative energies and Gibbs free energies at 165 °C of the four conformers at various levels of theory. We find in all cases that the s-*cis* pair of *anti*/*syn* conformers is predicted to be lower in energy than the s-*trans* pair by about 0.7–1.0 kcal/mol. Between the *anti* and *syn* conformers much smaller energy differences are calculated. Although these energy differences are too small to draw definite conclusions from, it is worth noticing that at all levels of calculations the *anti*/*syn* energy difference is consistently predicted to be much smaller

Table 1. Zero-Point Energy Corrected Energies (kcal/mol) and in Parentheses Gibbs Free Energies under Expansion Conditions (165 °C) of Conformers of Methyl 4-Hydroxycinnamate Calculated at Various Levels of DFT- and WF-Based Quantum Chemical Methods[a]

conformer	Δ*E* B3LYP	Δ*E* B3LYP +D	Δ*E* MP2	Δ*E* SCS-MP2
s-*cis* OH-*anti*	0.00	0.00	0.00	0.00
s-*cis* OH-*syn*	0.08 (0.04)	0.08 (0.04)	0.17 (0.46)[b]	0.10 (0.03)
s-*trans* OH-*anti*	0.96 (0.81)	0.90 (0.75)	0.73 (0.64)	0.66 (0.59)
s-*trans* OH-*syn*	0.96 (0.77)	0.91 (0.72)	0.74 (0.59)	0.68 (0.55)

[a]Reported with respect to energy of s-*cis* OH-*anti* conformer. [b]The reason that the relative Gibbs free energy of the s-*cis* OH-*syn* conformer increases compared to the zero-point energy corrected energy while it decreases for the other conformers is that the lowest-frequency mode in this conformer is found at ~40 cm^{-1} while in the other conformers its frequency is ~30 cm^{-1}.

dx.doi.org/10.1021/jp312624e | J. Phys. Chem. B 2013, 117, 4798–4805

for the s-*trans* than for the s-*cis* conformer. This is in agreement with the observed intensities in the (1 + 1′) RE2PI excitation spectrum shown in Figure 1 where it is observed that the *anti*/*syn* intensity ratio is larger for the s-*cis* conformer than for the s-*trans* conformer.

IR spectra predicted at various levels of theory for the s-*cis* OH-*syn*, s-*cis* OH-*anti*, and s-*trans* OH-*anti* conformers are depicted in Figures 3−5. To facilitate a comparison with the

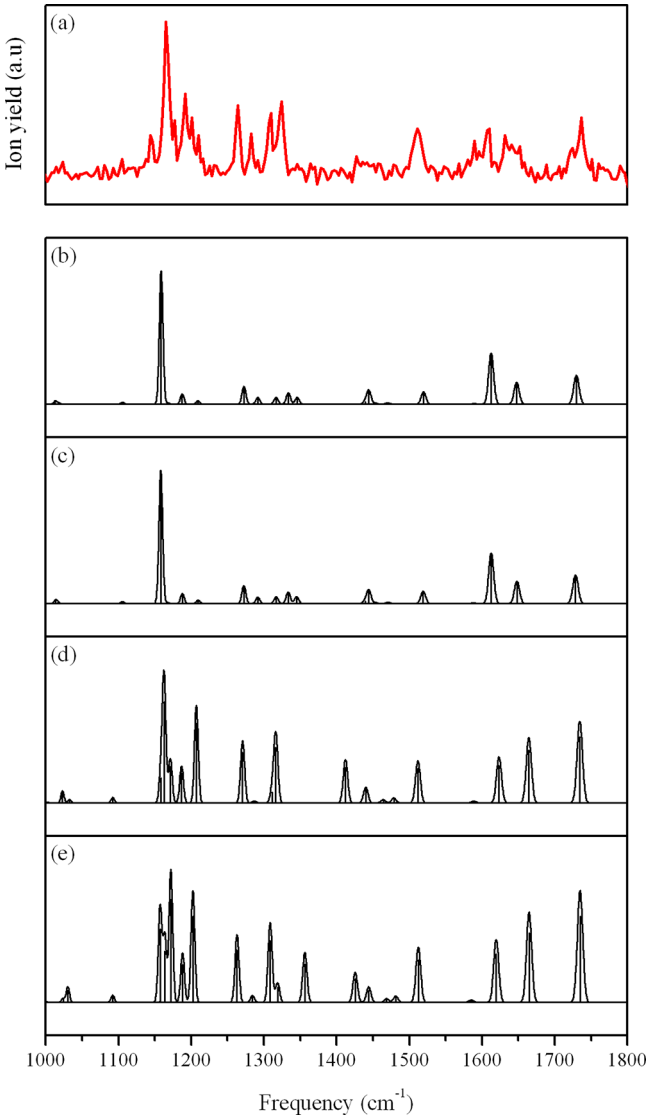

Figure 3. Observed and predicted IR spectra of the s-*cis* OH-*syn* conformer of OM*p*CA: (a) experimental IR−UV depletion spectrum; predicted spectrum at the (b) B3LYP, (c) B3LYP-D3, (d) MP2, and (e) SCS-MP2 level.

experimental spectra, the calculated infrared frequencies have been scaled with the appropriate method and basis set dependent scaling factors that have been prescribed.[26] Calculated stick spectra have been convoluted with a Gaussian band profile with a FWHM bandwidth that matches the spectral bandwidth of FELIX (0.5% of the frequency).

Because of its reliability and cost-effectiveness, DFT methods are nowadays commonly used to predict structures and vibrational spectra of medium- to large-sized molecular systems. A cursory comparison of the spectra calculated at the DFT/

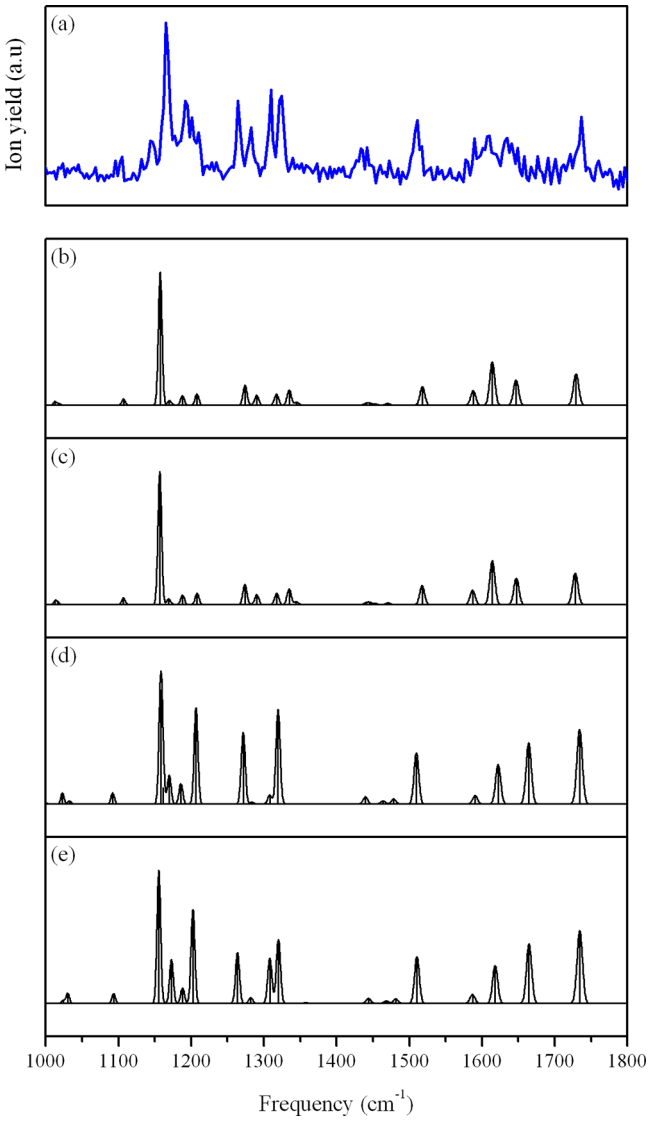

Figure 4. Observed and predicted IR spectra of the s-*cis* OH-*anti* conformer of OM*p*CA: (a) experimental IR−UV depletion spectrum; predicted spectrum at the (b) B3LYP, (c) B3LYP-D3, (d) MP2, and (e) SCS-MP2 level.

B3LYP level of theory (traces (b)) with the measured spectra shows excellent agreement as far as the frequencies of vibrational bands is concerned. However, with respect to their relative intensities larger deviations are observed, in particular when the activity of bands in the 1150−1350 cm^{-1} region is considered. In order to assess whether dispersion effects might account for these differences, calculations have been performed using the empirical dispersion correction introduced by Grimme[27] (DFT-D3). Traces (c) show that spectra obtained in this way are only marginally different from those obtained without dispersion correction, which is in line with the notion that DFT-D3 only corrects the long-range correlation.[28] It is thus expected to be of minor influence for molecules of the size of the presently considered chromophore.

The possible influence of electron correlation on the vibrational spectra was further investigated by MP2 calculations and an improved spin-component-scaled second-order Möller−Plesset theory (SCS-MP2) version developed by Grimme et al.[23] The latter method is believed to provide a better

dx.doi.org/10.1021/jp312624e | J. Phys. Chem. B 2013, 117, 4798−4805

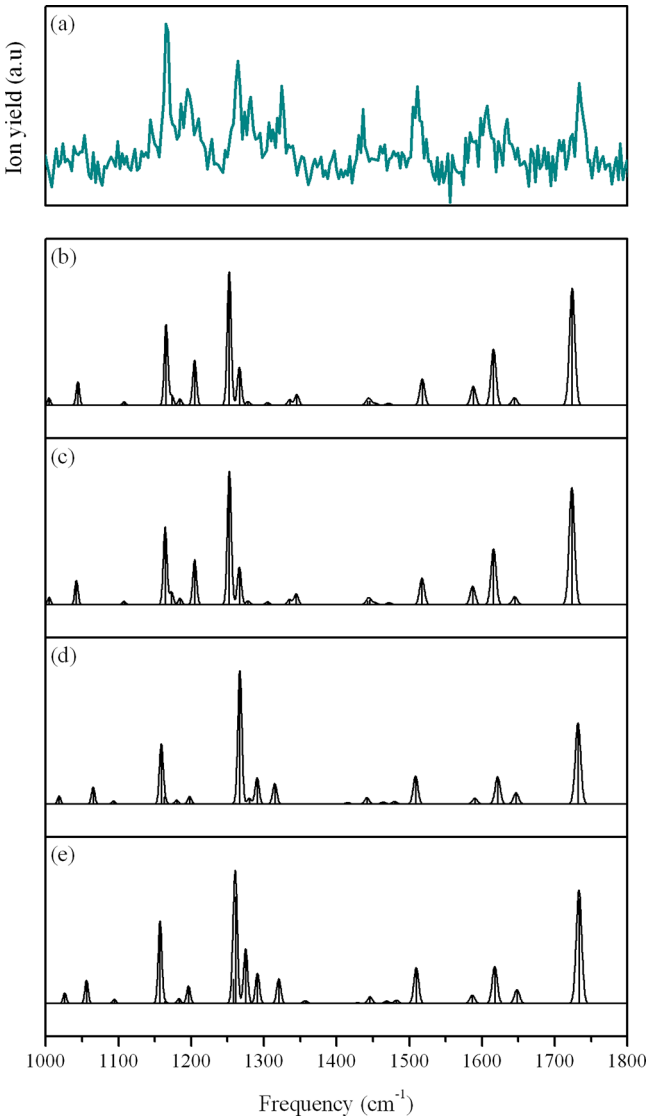

Figure 5. Observed and predicted IR spectra of the s-*trans* OH-*anti* conformer of OM*p*CA: (a) experimental IR−UV depletion spectrum; predicted spectrum at the (b) B3LYP, (c) B3LYP-D3, (d) MP2, and (e) SCS-MP2 level.

prediction of the normal modes because of the different scaling factors employed for second-order parallel and antiparallel spin pair correlation energies. Trace (d) in Figures 3−5 show that for the s-*cis* conformer the MP2-predicted spectra are significantly different from the DFT-predicted spectra. In particular the 1150−1350 cm^{-1} region, where appreciable intensity deviations between predicted and measured spectra were observed in the DFT calculations, now appears to be much more in line with the experimental spectra. Remarkably, we find for the s-*trans* conformer that the DFT- and MP2-predicted spectra are more similar, although below we will still conclude that also for this conformer MP2-predicted spectra match the experimental intensities better than the DFT-predicted ones. The use of SCS-MP2, on the other hand, does not lead to noteworthy changes in the spectra for either of the conformers as can be concluded from the comparison of traces (d) and (e) in Figures 3−5.

Comparison of the IR spectra predicted for the s-*cis* and s-*trans* conformers show a number of distinct differences that could serve as vibrational markers. In the 1300−1320 cm^{-1} region all levels of calculations predict that the s-*cis* conformer has a strong-intensity band of about the same intensity as the band around 1260 cm^{-1}. In the s-*trans* conformer this band is much weaker, and this frequency region is more dominated by the set of bands in the 1260−1280 cm^{-1} region. Similarly, we find in the 1000−1060 cm^{-1} region a number of low-intensity bands. For the s-*trans* conformer three bands are predicted to occur with the strongest activity around 1050 cm^{-1}, while for the s-*cis* conformer two bands near 1020 and 1100 cm^{-1} are expected. The MP2 calculations, finally, predict for the s-*cis* conformers the presence of a band of medium intensity in the 1650 cm^{-1} region which shifts to a lower frequency and has a reduced intensity in the s-*trans* conformers. However, this trend is less clear in the DFT calculations.

Whereas the comparison between the IR spectra of s-*cis* and s-*trans* shows that in a number of frequency regions appreciable differences occur, the differences between the IR spectra of the OH-*anti* and OH-*syn* conformers are not as straightforward. Since the OH-group is attached to the end of the phenyl ring, one might expect differences in the frequency region associated with deformations of the phenyl ring coupled to the deformations of the hydroxyl group. Indeed, inspection of the predicted spectra reveals three bands that are different in the two types of conformers and that involve such deformations. For the *syn* conformer, a band of medium intensity is predicted around 1350 cm^{-1} which involves the double-bond stretch of the phenyl ring and the OH bend, and which is absent in the *anti* spectra. Similarly, the calculations predict a weak band associated with the CH bend of the phenyl ring coupled with the CC stretch and OH bend in the 1430 cm^{-1} region of the *syn* conformer which is blue-shifted and reduced in intensity for the *anti* conformer. Finally, in the 1580 cm^{-1} region a band involving the CC stretch and OH bend is predicted to be more intense for the *anti* conformer than for the *syn* conformer.

Careful inspection of the experimental IR spectra leads to the conclusion that these spectra indeed show small but distinct differences in the frequency regions discussed above. The difference between s-*cis* and s-*trans* is most clearly observed in the 1310−1330 cm^{-1} region where s-*cis* shows two bands at 1310 and 1325 cm^{-1}, while the 1310 cm^{-1} band is much weaker for s-*trans*. For the *syn-anti* distinction the band observed for the *syn* conformer at 1346 cm^{-1} and the band observed at 1577 cm^{-1} for the *anti* conformer are the most clear markers. The full comparison between experiment and theory leads to the assignment of experimental bands as reported in Table 2.

Under biological conditions, the PYP chromophore is influenced by its environment. It is therefore of interest to see to what extent this influence is reflected in IR spectra. As a first step toward mimicking a biological environment, we have therefore recorded IR−UV depletion spectra for the OM*p*CA-H_2O cluster. Previous studies in the 3 μm region of the spectrum have shown that this part of the spectrum changes significantly: on account of hydrogen bonding between the phenolic OH and the complexed water the OH stretch frequency is reduced by some 155 cm^{-1}.[12] Figure 2, traces d and e, shows IR−UV depletion spectra at UV excitation wavelengths that previously have been assigned to the $S_1 \leftarrow S_0$ origin transitions of the s-*cis* and s-*trans* conformers. For the cluster the *syn*/*anti* splitting is much smaller than for the bare molecule.[12] The spectra in Figure 2d and e therefore contain unresolved contributions from the *syn* and *anti* conformers. Originally, the band at 32 078.0 cm^{-1} was assigned to the s-

dx.doi.org/10.1021/jp312624e | J. Phys. Chem. B 2013, 117, 4798−4805

Table 2. Assignment and Relative Intensities[a] of Vibrational Bands in Experimental IR Spectra of the s-*cis* OH-*syn*, s-*cis* OH-*anti*, and s-*trans* OH-*anti* Conformers of OM*p*CA

frequency (cm^{-1})						
s-*cis* OH-*syn*	intensity	s-*cis* OH-*anti*	intensity	s-*trans* OH-*anti*	intensity	assignment[b]
1014	vw	1017	vw	1023	w	H−C═C−H oop bend
1023	vw	1023	vw	1053	w	methyl ester CC stretch, O−CH_3 stretch
1104	vw	1105	vw	1099	w	═C−H bend (aro), O−H bend
1144	w	1147	w	1144	w	CH_3 twisting (in-plane axis)
1165	vs	1165	vs	1165	vs	C−O stretch, ═C−H bend (aro), O−H bend
1177	w	1177	w	1174	w	C−O stretch, ═C−H bend (aro), O−H bend
1192	s	1192	s	1186	s	CH_3 wagging
1201	w	1201	w	1195	s	═C−H bend (aro), aro-C stretch, CH bend
1210	w	1210	w	1210	w	═C−H bend (aro), aro-C stretch, CH bend
1264	w	1264	s	1264	vs	C−O stretch (hydroxyl), C−H bend (aro)
1282	w	1282	w	1282	s	C−C stretch (aro), C−H bend
1310	w	1310	s	1306	w	C═C−H bend
1325	s	1325	s	1325	s	C−H bend (aro)
1346	vw	1345	vw	1352	w	C═C stretch (ring), C−H bend, O−H bend
1427	vw	1427	vw	1430	w	C═C stretch (ring), C−H bend, O−H bend, CH_3 umbrella
1442	vw	1433	vw	1436	s	CC stretch (ring), C−H bend, O−H bend
1460	vw	1460	vw	1462	w	CH_3 scissoring, CH_3 rocking
1478	vw	1472	vw	1478	w	CH_3 scissoring
1511	w	1511	w	1511	s	C−H bend (ring), C−C stretch
1580	vw	1577	vw	1583	w	CC stretch (ring), O−H bend (hydroxyl)
1610	w	1610	w	1607	s	CC stretch (ring)
1640	w	1640	w	1634	w	C═C stretch
1736	w	1736	w	1733	s	C═O stretch

[a]vw = very weak (intensity ≤0.25), w = weak (0.25 < intensity ≤0.5), s = strong (0.5 < intensity ≤0.75), vs = very strong (intensity >0.75). [b]oop = out of plane, aro = aromatic.

trans conformer of the complex and the band at 32 142.0 to the s-*cis* conformer. Inspection of the 1310−1330 cm^{-1} region shows that for probing at 32 078.0 cm^{-1} two bands of equal intensity are present while for probing at 32 142.0 cm^{-1} the higher-frequency band has a considerably larger intensity. Above, we have seen that these intensity distributions are characteristic for the s-*cis* and s-*trans* conformers, respectively. We therefore conclude that the original assignment should be reversed. For the bare molecule the s-*cis*/s-*trans* splitting is 170.2 cm^{-1}.[29] We now thus find that in the complex this splitting is reduced by 106.2 to 64.0 cm^{-1}. This is much more in line with a priori expectations than the original assignment which would have implied a change in splitting by 234.2 cm^{-1}, i.e., a change that would be larger than the original splitting. Comparison of the spectra of the complex with the spectra of the bare molecule does not reveal significant differences. Theoretical calculations of the IR absorption spectra of the complex indeed give rise to spectra that very much resemble those of the bare chromophore (see Supporting Information) and support the above assignment of the two hydrates. One thus has to conclude that the influence of the water molecule on the electronic structure that so clearly comes forward in the 3 μm region of the IR spectrum and in electronic excitation studies[12] is considerably less evident in the mid-IR region.

Apart from the IR−UV depletion spectra on isolated OM*p*CA, Figure 2 depicts as well the IR absorption spectrum of OM*p*CA dissolved in chloroform (Figure 2f). Taking into account that the bands in the gas-phase spectra are progressively broader for increasing frequencies due to the frequency-dependent spectral line width of FELIX while the spectral line width in the solvent spectrum is constant, the solution and gas-phase spectra are very similar. Interestingly, we find that in solution the carbonyl stretch vibration is significantly red-shifted and broadened, in agreement with the notion that the vibrational frequency of this mode is dependent on the properties of the solvent such as its dielectric constant and on effects from hydrogen bonding and donor−acceptor interactions.[30,31] From electronic spectroscopy studies on chromophores of PYP and on the complete PYP protein, it has been suggested that the protein pocket is hydrophobic,[32] and that gas-phase studies are thus most relevant to the biological situation. The present IR studies indicate that the carbonyl stretch frequency might be used as an additional and alternative probe for assessing the extent to which the protein pocket environment influences the chromophore of PYP.

CONCLUSIONS

In the present study we have employed various UV and IR double resonance methods to disentangle the conformational heterogeneity of methyl 4-hydroxycinnamate, a model compound for the light-absorbing part of the photoactive yellow protein. Such studies are the more relevant in view of the observed dependence of the photophysical properties on the structural parameters of the chromophore. In the spectroscopic experiments, four different species can be identified that have been assigned to specific conformers on the basis of a careful comparison of experimental IR absorption spectra with theoretically predicted spectra. The calculated energy differences between these conformers are within the accuracy of the theoretical methods and thus do not warrant their use for assigning conformers. Nevertheless, we find that the assignment deduced from the IR spectra follows the calculated stabilities of the conformers. The vibrational markers that have been identified for the conformers of the bare molecule have led

dx.doi.org/10.1021/jp312624e | J. Phys. Chem. B 2013, 117, 4798−4805

to the conclusion that the original assignment of the s-*cis* and s-*trans* conformers of the complex of methyl 4-hydroxycinnamate with water should be reversed.

With respect to the IR spectra of the *syn* and *anti* conformers, one would a priori have expected small differences as is indeed observed in the experiments. However, for the s-*cis* and s-*trans* conformers the present study has shown that their observed IR spectra are much more similar than what would have been expected on the basis of the quantum chemical calculations. Moreover, the present study has shown that the inclusion of dynamic electron correlation by MP2 calculations has a surprisingly different effect on the calculated spectra of these two conformers. The experimental IR spectra obtained in the present study may thus serve as a benchmark to determine which aspects of quantum chemical calculations need to be improved to come to a better agreement between experimental and theoretical IR spectra. In the same way, we hope that the finer details in the reported high-resolution excitation spectra—such as the different *syn*/*anti* splitting for the s-*cis* and s-*trans* conformers, the different excitation energy order of the *syn*/*anti* pair for the s-*cis* and s-*trans* conformers, and the difference in red shift of the excitation energy of the s-*cis* and s-*trans* conformers upon complexation with water—will provide further incentive for detailed high-quality quantum chemical calculations on the consequences of small structural changes on the electronic structure of ground and electronically excited states.

■ ASSOCIATED CONTENT

Supporting Information

A more extensive discussion on the influence of anharmonicity by means of a comparison between IR spectra calculated within the harmonic and anharmonic approximation, and a comparison between experimental IR spectra and spectra predicted for various conformers of the OMpCA–H_2O cluster. This material is available free of charge via the Internet at http://pubs.acs.org.

■ AUTHOR INFORMATION

Corresponding Author

*E-mail: w.j.buma@uva.nl.

Notes

The authors declare no competing financial interest.

■ ACKNOWLEDGMENTS

This work was supported by The Netherlands Organization for Scientific Research (NWO). We thank the staff of FELIX for their support during the experiment. S.A. thanks the Deutsche Akademie der Naturforscher Leopoldina—German National Academy of Sciences for a Leopoldina research fellowship (grant no. LPDS 2011-18).

■ REFERENCES

(1) Meyer, T. E. *Biochim. Biophys. Acta* **1985**, *806*, 175.
(2) Meyer, T. E.; Yakali, E.; Cusanovich, M. A.; Tollin, G. *Biochemistry* **1987**, *26*, 418.
(3) Hellingwerf, K. J.; Hendriks, J.; Gensch, T. *J. Phys. Chem. A* **2003**, *107*, 1082.
(4) Ko, C.; Levine, B.; Toniolo, A.; Manohar, L.; Olsen, S.; Werner, H.-J.; Martinez, T. J. *J. Am. Chem. Soc.* **2003**, *125*, 12710.
(5) Li, Q.-S.; Fang, W.-H. *Chem. Phys.* **2005**, *313*, 71.
(6) Gromov, E. V.; Burghardt, I.; Koppel, H.; Cederbaum, L. S. *J. Phys. Chem. A* **2005**, *109*, 4623.
(7) Ryan, W. L.; Gordon, D. J.; Levy, D. H. *J. Am. Chem. Soc.* **2002**, *124*, 6194.
(8) Nielsen, I. B.; Boye-Peronne, S.; El Ghazaly, M. O. A.; Kristensen, M. B.; Nielsen, S. B.; Andersen, L. H. *Biophys. J.* **2005**, *89*, 2597.
(9) Lee, I.-R.; Lee, W.; Zewail, A. H. *Proc. Natl. Acad. Sci. U.S.A.* **2006**, *103*, 258.
(10) Smolarek, S.; Vdovin, A.; Perrier, D. L.; Smit, J. P.; Drabbels, M.; Buma, W. J. *J. Am. Chem. Soc.* **2010**, *132*, 6315.
(11) de Groot, M.; Gromov, E. V.; Köppel, H.; Buma, W. J. *J. Phys. Chem. B* **2008**, *112*, 4427.
(12) Smolarek, S.; Vdovin, A.; Tan, E. M. M.; de Groot, M.; Buma, W. J. *Phys. Chem. Chem. Phys.* **2011**, *13*, 4393.
(13) Shimada, D.; Kusaka, R.; Inokuchi, Y.; Ehara, M.; Ebata, T. *Phys. Chem. Chem. Phys.* **2012**, *14*, 8999.
(14) Tan, E. M. M.; Amirjalayer, S.; Bakker, B.; Buma, W. J. *Faraday Discuss.* **2013**, DOI: 10.1039/C2FD20139A.
(15) de Groot, M.; Buma, W. J.; Gromov, E. V.; Burghardt, I.; Köppel, H.; Cederbaum, L. S. *J. Chem. Phys.* **2006**, *125*, 204303.
(16) Morgan, P. J.; Mitchell, D. M.; Pratt, D. W. *Chem. Phys.* **2008**, *347*, 340.
(17) Smolarek, S.; Vdovin, A.; Rijs, A. M.; van Walree, C. A.; Zgierski, M. Z.; Buma, W. J. *J. Phys. Chem. A* **2011**, *115*, 9399.
(18) Rijs, A. M.; Kay, E. R.; Leigh, D. A.; Buma, W. J. *J. Phys. Chem. A* **2011**, *115*, 9669.
(19) Wilson, A. K.; Woon, D. E.; Peterson, K. A.; Dunning, T. H. *J. Chem. Phys.* **1999**, *110*, 7667.
(20) Becke, A. D. *J. Chem. Phys.* **1993**, *98*, 5648.
(21) Lee, C.; Yang, W.; Parr, R. G. *Phys. Rev. B* **1988**, *37*, 785–789.
(22) Grimme, S.; Antony, J.; Ehrlich, S.; Krieg, H. *J. Chem. Phys.* **2010**, *132*, 154104.
(23) Gerenkamp, M.; Grimme, S. *Chem. Phys. Lett.* **2004**, *392*, 229.
(24) TURBOMOLE V6.1, 2009; a development of the University of Karlsruhe and Forschungszentrum Karlsruhe GmbH, 1989–2007; TURBOMOLE GmbH since 2007. http://www.turbomole.com (accessed July 8, 2012).
(25) Rodrigo, C. P.; James, W. H.; Zwier, T. S. *J. Am. Chem. Soc.* **2011**, *133*, 2632.
(26) J.P. Merrick, J. P.; Moran, D.; Radom, L. *J. Phys. Chem. A* **2007**, *111*, 11683.
(27) Grimme, S. *J. Comput. Chem.* **2004**, *25*, 1463.
(28) Schwabe, T.; Grimme, S. *Acc. Chem. Res.* **2008**, *41*, 569.
(29) Calculated as the difference between the average of the *syn*/*anti* excitation energies of the s-*cis* and s-*trans* conformers.
(30) Jagesar, D. C.; Hartl, F.; Buma, W. J.; Brouwer, A. M. *Chem.—Eur. J.* **2008**, *14*, 1935.
(31) Fawcett, W. R.; Kloss, A. A. *J. Phys. Chem.* **1996**, *100*, 2019.
(32) Nielsen, I. B.; Boye-Peronne, S.; El Ghazaly, M. O. A.; Kristensen, M. B.; Nielsen, S. B.; Andersen, L. H. *Biophys. J.* **2005**, *89*, 2597.